Optical Production of Ultracold Polar Molecules

Jeremy M. Sage,[1] Sunil Sainis,[1] Thomas Bergeman,[2] and David DeMille[1]
[1]*Department of Physics, Yale University, New Haven, Connecticut 06520, USA*
[2]*Department of Physics and Astronomy, SUNY, Stony Brook, New York 11794-3800, USA*

(Received 29 December 2004; published 23 May 2005)

We demonstrate the production of ultracold polar RbCs molecules in their vibronic ground state, via photoassociation of laser-cooled atoms followed by a laser-stimulated state transfer process. The resulting sample of $X^1\Sigma^+(v = 0)$ molecules has a translational temperature of $\sim$100 μK and a narrow distribution of rotational states. With the method described here it should be possible to produce samples even colder in all degrees of freedom, as well as other bialkali species.

DOI: 10.1103/PhysRevLett.94.203001 PACS numbers: 32.80.Pj, 39.25.+k, 33.70.Ca, 33.80.Wz

Samples of ultracold, polar molecules (UPMs) can provide access to new regimes in many phenomena. Ultracold temperatures allow trapping, and polarity can be used to engineer large, anisotropic, and tunable interactions between molecules. These features make UPMs attractive as qubits for quantum computation [1], as building blocks for novel many-body systems [2], and for the study of chemistry in the ultracold regime [3]. UPMs also could be used as uniquely sensitive probes of phenomena beyond the standard model of particle physics [4].

Methods such as buffer-gas cooling [5], Stark-slowing [6], billiardlike collisions [7], and velocity filtering [8] have produced samples of polar molecules at temperatures of $\sim$1–100 mK. Formation of heteronuclear molecules from precooled atoms via photoassociation (PA) [9–12] or Feshbach resonance techniques [13] promises access to much lower temperatures. However, these processes leave molecules in highly excited vibrational levels, which have vanishingly small polarity [14] and are unstable to collisions [15,16]. The possibility of transferring such molecules to their vibronic ground state, via optical processes such as stimulated Raman transitions, has been discussed extensively (see, e.g., [1,17–20]); however, insufficient data on the structure of experimentally accessible molecules has made it difficult to identify specific pathways for efficient transfer.

Here we report the production of UPMs via PA of laser-cooled Rb and Cs atoms, followed by a two-step stimulated emission pumping (SEP) process. This yields RbCs molecules in their absolute vibronic ground state $X^1\Sigma^+(v = 0)$. These polar molecules (calculated electric dipole moment $\mu \approx 1.3$ D [21]) have a translational temperature of $\sim$100 μK. The distribution of rotational states is also quite narrow, so the resulting sample of $X^1\Sigma^+$ state molecules is cold in all degrees of freedom.

Figure 1 shows the methods by which we produce and detect UPMs. A pair of colliding, ultracold Rb and Cs atoms is photoassociated; i.e., the pair absorbs a photon and is driven to an electronically excited molecular level [22]. This level decays rapidly, with a branching fraction of $\sim$7% into the long-lived $a^3\Sigma^+(v = 37)$ level [9]. After a period of PA, a resonant laser pulse (“pump” pulse) transfers these metastable, vibrationally excited molecules to an intermediate, electronically excited state (i). The population of state i is monitored by applying an intense laser pulse (“ionization” pulse), with a frequency chosen to selectively form RbCs$^+$ molecular ions. We detect these ions using time-of-flight mass spectroscopy.

To produce $X(v = 0)$ molecules, a second tunable laser pulse (“dump” pulse), arriving just after the pump pulse, resonantly drives molecules in state i to the $X(v = 0)$ (or, for diagnostic purposes, $v = 1$) state. Transfer to the $X(v = 0, 1)$ states is indicated by a depletion of the i state population. This method [23] generally works well, but is complicated by the presence of additional resonant features associated with transitions from state i upward into other, spectrally uncharacterized excited states.

We thus employ a second method to directly detect the RbCs $X(v = 0, 1)$ molecules. After the dump pulse, the population of state i is allowed to decay for several times its spontaneous emission lifetime, leaving essentially no population in this level. Next a third pulse (“reexcitation” pulse), identical in frequency to the dump, drives the stable $X^1\Sigma^+(v = 0, 1)$ molecules back into state i, where they are detected via ionization as before. The ion signal is monitored as the frequency of the identical dump and reexcitation pulses is scanned; a peak in this signal indicates that molecules have been resonantly transferred to the $X^1\Sigma^+(v = 0, 1)$ states by the dump pulse, then back to the i state by the reexcitation pulse. The definitive signatures of UPM production are resonances at the exact frequencies predicted by earlier spectroscopy of the $a^3\Sigma^+$, i [9,18], and $X^1\Sigma^+$ levels [24].

The state i is in the manifold of levels associated with the overlapping electronic states $c^3\Sigma^+$, $B^1\Pi$, and $b^3\Pi$. Specifically, the states chosen for i have predominantly $c^3\Sigma_1^+$ character, with small admixtures of $B^1\Pi_1$ (due to spin-orbit coupling) and $b^3\Pi_1$ (due to both spin-orbit and nonadiabatic couplings). The mixed c/B state composition of i is crucial to the technique (the small b state admixture is incidental). The $c^3\Sigma^+$ component of the i state has reasonable Franck-Condon (FC) overlap with the initial

$a^3\Sigma^+(v = 37)$ state, due to the near coincidence of the inner turning point of the $a^3\Sigma^+$ potential with the minimum of the $c^3\Sigma^+$ potential [9,18]. The $B^1\Pi$ component of state i circumvents the usual selection rule forbidding transitions from the initial triplet state a to the final singlet state X. Moreover, the minima of the $B^1\Pi$ and $X^1\Sigma^+$ potentials nearly coincide, leading to large FC factors for transfer to the $X(v = 0)$ level.

The apparatus is similar to that described in our earlier work [9]. Briefly, ^{85}Rb and ^{133}Cs atoms were cooled and collected in a dual-species, forced dark SPOT (spontaneous-force optical trap) magneto-optical trap (MOT) [25–27]. The atomic density n and atom number N were $n_{\mathrm{Rb}} = 1 \times 10^{11}\ \mathrm{cm}^{-3}$, $N_{\mathrm{Rb}} = 2 \times 10^8$, and $n_{\mathrm{Cs}} = 3 \times 10^{11}\ \mathrm{cm}^{-3}$, $N_{\mathrm{Cs}} = 3 \times 10^8$. The temperature of both species was $\sim 75\ \mu$K. The PA laser had an intensity of $\sim 3\ \mathrm{kW/m^2}$, and its frequency was locked to an $\Omega = 0^-$, $J^P = 1^+$ level, located $38.02\ \mathrm{cm}^{-1}$ below the Rb $5S_{1/2}(F = 2)$ + Cs $6P_{1/2}(F = 3)$ atomic asymptote. This laser was applied for the 100 ms period between pump pulses (though the steady-state number of molecules in the detection region was reached within ~10 ms [25]).

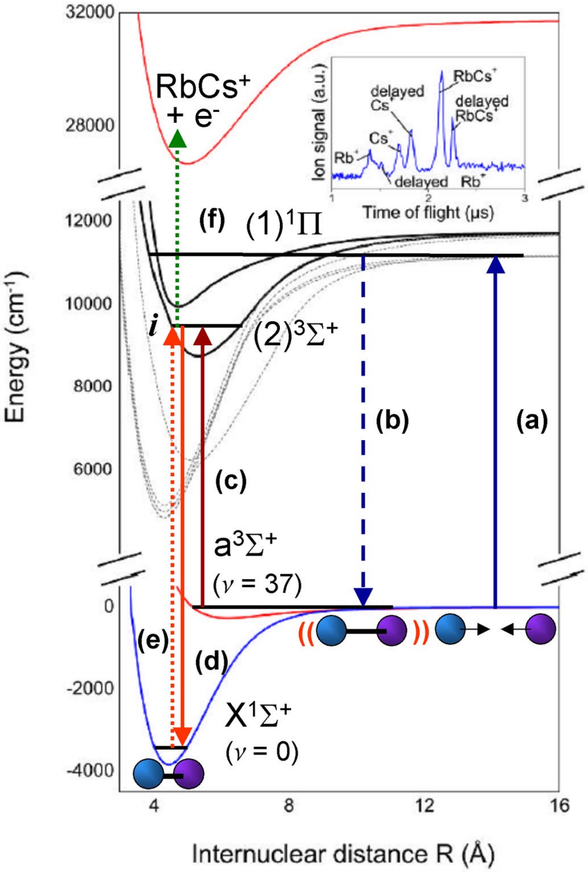

FIG. 1 (color online). Formation and detection processes for ultracold ground state RbCs. (a) Colliding atom pairs are excited into bound RbCs* molecules, which (b) decay prominently into the $a^3\Sigma^+(v = 37)$ state. (c) Metastable $a(v = 37)$ molecules are excited to level i, then (d) stimulated into the $X^1\Sigma^+(v = 0)$ state. The molecules are detected directly by (e) driving them back to the original excited level and (f) ionizing them, or indirectly by detecting the depletion of the i level population [where only (f) is needed]. Inset: a typical time-of-flight mass spectrum showing the direct detection of $X(v = 0)$ molecules. The ion signal, averaged over 200 shots, is plotted vs delay time after the ionizing pulse. The delayed RbCs$^+$ peak signifies ground state molecule production.

All other laser light consisted of pulses with ~5 ns duration and ~3 mm diameter. The pump pulse was generated from a tunable dye laser operating from $18\,100$–$18\,600\ \mathrm{cm}^{-1}$ at a 10 Hz repetition rate with a spectral linewidth of $\sim 0.05\ \mathrm{cm}^{-1}$. This output was sent through a H_2 Raman cell; the second Stokes order (downshifted by $2 \times 4155.25\ \mathrm{cm}^{-1}$) was separated to form the pump pulse, with a typical pulse energy of 150 μJ and frequency from 9800–$10\,300\ \mathrm{cm}^{-1}$. The dump and reexcitation pulses were generated using an additional dye laser (the "red" laser) operating from $13\,500$–$14\,000\ \mathrm{cm}^{-1}$ with a spectral linewidth of $\sim 0.2\ \mathrm{cm}^{-1}$; each had a typical pulse energy of 20 μJ. The ionizing pulse (at 532 nm) was derived from the second harmonic of the Nd-doped yttrium aluminum garnet laser used to pump the dye lasers, and had a pulse energy of 750 μJ.

The red and ionizing beams were spatially combined using a dichroic mirror with the ionizing pulse propagating 4 ns behind the red pulse. These combined beams were sent through a beam splitter. In one half of the split two-color beam, the optical path length was adjusted such that the red dump pulse reached the molecules 7 ns after the pump pulse. The other half of the two-color beam was sent through a 22 m long multimode optical fiber; with this delay, the red reexcitation pulse arrived 110 ns after the dump pulse.

Ions were detected using a channeltron located ~3 cm from the atoms. The output current yields a time-of-flight mass spectrum (see Fig. 1). The temperature of the molecules in the $a^3\Sigma^+$ state was measured to be $\sim 100\ \mu$K, as described in Ref. [25]. The scattering of two photons necessary to transfer the population to the $X(v = 0)$ state should not cause significant heating.

For a particular choice of state i, we scanned the frequency of the red laser through the predicted energy splitting between the chosen level and the $X^1\Sigma^+(v = 0, 1)$ states. We observed transfer to the ground states via several of these levels. Results are shown for three such intermediate states i, consecutive in energy, in Fig. 2.

The locations of the resonant features are in excellent agreement with the known $X(v = 0) - (v = 1)$ splitting [24] and with our measured splitting of the i state levels. In Fig. 2(c), a scan over the region between the $v = 0$ and $v = 1$ resonances shows features only at the predicted locations. As a cross-check, we also deliberately chose as state i the $\Omega = 0^-$ component of a mixed $c^3\Sigma^+/b^3\Pi$ level. Here, selection rules rigorously prevent coupling to the $X^1\Sigma^+$ state, and as expected we observe no evidence for transfer. Finally, we determined the strength of the

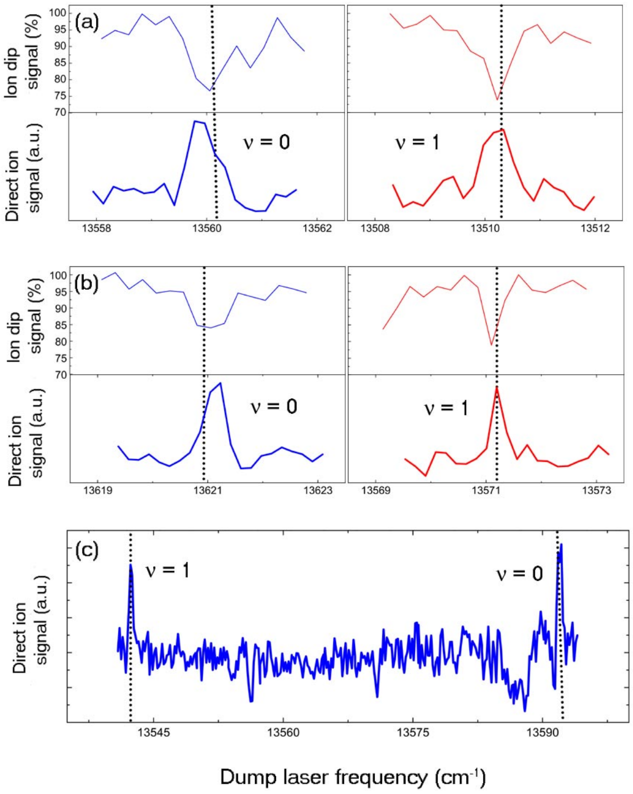

FIG. 2 (color online). Observation of $X^1\Sigma^+(v = 0, 1)$ state molecules. Results are shown for i state depletion (upper) and direct detection (lower) for three consecutive states i, located at energies of (a) 9754.26 cm^{-1}, (b) 9814.60 cm^{-1}, and (c) 9786.10 cm^{-1} above the $a^3\Sigma^+(v = 37)$ state. In (c), the region between the $v = 0$ and $v = 1$ resonances is shown to have no additional features for direct detection. The dotted lines indicate the predicted dump laser frequency for the desired transition. All frequencies are measured to a 0.05 cm^{-1} accuracy. All data are averaged over 100 pulses.

$i - X$ transitions by increasing the red laser pulse energy until the resonant features broadened. The observed saturation pulse energies (typically $\sim 30\ \mu\mathrm{J}$) agree qualitatively with those predicted from calculated FC factors and electronic transition moments [18].

Our $X^1\Sigma^+$ molecular sample is of high purity with respect to the vibrational degree of freedom. State i is dominantly triplet in character, and thus the probability of uncontrolled spontaneous decay to the $X^1\Sigma^+$ state during the SEP step is extremely small. Using our earlier analysis of the mixed $c/B/b$ state structure [18], we calculated branching ratios for decay of the i states. While these calculations are only qualitative (due to our incomplete knowledge of the relevant state wave functions), they indicate that the total population in all other vibrational levels of the $X^1\Sigma^+$ state is only $\sim 1\%$ of the population driven into the $v = 0$ level. (Of course, there remains a substantial background of $a^3\Sigma^+$ molecules.)

The rotational and hyperfine state distribution of the $X(v = 0)$ molecules is determined by selection rules and by the laser spectral resolution. Hyperfine structure (hfs) is unresolved in all stages of the process, and hence the nuclear spin degrees of freedom are unconstrained; however, the initial PA step selects a level with rotation and parity quantum numbers $J^P = 1^+$. The three subsequent photons involved in the transfer to the X state (one in spontaneous emission and two in the SEP) leave the molecule in a state of odd parity, and can add up to 3 units of angular momentum. Noting that $P = (-1)^J$ for the $X^1\Sigma^+$ state, this suggests that only $J = 1, 3$ could be populated in $X(v = 0)$. However, the molecule could also acquire rotational angular momentum from the nuclear spins if the hfs and rotation are coupled. This can add up to $I_{\mathrm{Rb}} + I_{\mathrm{Cs}} = 6$ units of rotation (here I_x is the nuclear spin of species x), resulting in a range of rotational states of up to $J = 1$, 3, 5, 7, 9.

We derive a bound on the spread of populated rotational levels from the absence of large spectral shifts of the observed resonances from the predicted $J = 1$ lines. Our observations deviate by no more than 0.3 cm^{-1} from these predictions, which have an uncertainty of ± 0.6 cm^{-1} [18]. Using the known rotational constant $B_e = 0.017$ cm^{-1} [24], we conclude that, at most, $J = 1$, 3, 5, and 7 are populated. However, the spectral width of the dump and reexcitation resonances suggests an even narrower rotational distribution. A typical linewidth of 0.18 cm^{-1} (obtained by subtracting, in quadrature, our laser linewidth from the measured resonance width) agrees well with the predicted 0.17 cm^{-1} splitting between the $J = 1$ and 3 levels. This suggests that the hfs-rotation coupling may be weak, and that, indeed, only two rotational levels ($J = 1$ and 3) are populated.

In future work, we expect to produce molecules in a single rotational level by using transform-limited laser pulses capable of resolving rotational structure. State selection of hfs may also be possible by the use of spin-polarized atoms and hfs-resolved transitions for PA and state transfer. This would also increase the rate of $X(v = 0)$ molecule production, since currently the spread of population among hfs sublevels in the $a(v = 37)$ state limits the fraction available for transfer to the i state.

The current efficiency of the SEP process is $\sim 6\%$. This is determined by the measured $\sim 25\%$ dump and reexcitation efficiencies and inference of a similar pump efficiency (due to the comparable red and pump laser linewidths). This low value is expected due to the sparse comblike spectral structure typical of pulsed lasers with multiple longitudinal modes [28], such as those used here. This structure implies that we would need to broaden the transitions considerably in order to achieve the theoretical maximum 25% transfer efficiency for SEP with our current lasers. In future work, by using a stimulated Raman adiabatic passage technique with transform-limited laser pulses [29,30], the $a(v = 37)$ to $X(v = 0)$ transfer efficiency could approach 100%.

We detect ~ 1 ion per pulse after reexcitation. This indicates production of $\sim 5 \times 10^2$ UPMs/s, subject to uncertainties (estimated at a factor of ~2 overall) in the channeltron gain and ionization efficiency [31]. The UPM production rate is consistent with expectations [25] based on the PA rate (after scaling for lower MOT densities), the rate at which molecules leave the detection region after formation (time constant ~10 ms [25]), and the SEP transfer efficiency. Note that no attempt was made to optimize the MOT densities which govern the PA rate, and hence the UPM production rate, in these experiments.

This method for UPM production should be quite general. Mixing of the $c^3\Sigma^+$ and $B^1\Pi$ levels, as well as the favorable location of the potential curves, is present in all bialkali dimers [19]. Although such spin-orbit mixing increases with the mass of the molecules [32], it may be sufficiently large even for the lightest heteronuclear bialkali (LiNa). Also, the SEP method is fairly insensitive to the initial vibrational state and completely insensitive to molecular temperature. Thus, higher phase space densities of UPMs could be produced by photoassociating colder atoms or by starting with molecules formed by Feshbach resonance in a single $a^3\Sigma^+$ level [13].

We believe that the method described here can be used to produce substantial samples of trapped UPMs. Far-detuned optical dipole traps [33] can trap atoms [34,35], vibrationally excited molecules [36], and $X(v = 0)$ molecules [37]. Excited molecules formed in such a trap could be efficiently transferred to their absolute rovibrational ground state as described here. The number of trapped UPMs produced in this way will depend on the initial atomic conditions, the rate of collisional quenching of excited molecules, etc. However, the efficiency of the population-transfer process demonstrated here makes us optimistic that large numbers of UPMs will be available.

In summary, we have produced ultracold polar RbCs molecules in their ground vibronic state. The optical transfer technique used here should be applicable to other bialkali molecules. Translational temperatures limited only by atomic cooling methods should be achievable, and with available technology population of a single rovibronic state with high purity should be possible. This opens a route to the study and manipulation of polar molecules in the ultracold regime.

We thank A. J. Kerman for crucial contributions to earlier stages of this work and R. C. Hilborn for the loan of essential equipment. We acknowledge support at Yale from NSF Grant No. DMR0325580, the David and Lucile Packard Foundation, and the W. M. Keck Foundation, as well as at Stony Brook from NSF Grant No. PHY0354211 and the U.S. Office of Naval Research.

---

[1] D. DeMille, Phys. Rev. Lett. **88**, 067901 (2002).

[2] M. A. Baranov *et al.*, Phys. Rev. A **66**, 013606 (2002); K. Goral, L. Santos, and M. Lewenstein, Phys. Rev. Lett. **88**, 170406 (2002).

[3] E. Bodo, F. A. Gianturco, and A. Dalgarno, J. Chem. Phys. **116**, 9222 (2002).

[4] M. Kozlov and L. Labzowsky, J. Phys. B **28**, 1933 (1995); J. J. Hudson *et al.*, Phys. Rev. Lett. **89**, 023003 (2002); D. DeMille, Bull. Am. Phys. Soc. **49**, 97 (2004).

[5] J. D. Weinstein *et al.*, Nature (London) **395**, 148 (1998).

[6] H. L. Bethlem *et al.*, Nature (London) **406**, 491 (2000).

[7] M. S. Ellioff, J. J. Valentini, and D. W. Chandler, Science **302**, 1940 (2003).

[8] S. A. Rangwala *et al.*, Phys. Rev. A **67**, 043406 (2003).

[9] A. J. Kerman *et al.*, Phys. Rev. Lett. **92**, 153001 (2004).

[10] M. W. Mancini *et al.*, Phys. Rev. Lett. **92**, 133203 (2004).

[11] C. Haimberger *et al.*, Phys. Rev. A **70**, 021402(R) (2004).

[12] D. Wang *et al.*, Phys. Rev. Lett. **93**, 243005 (2004).

[13] S. Inouye *et al.*, Phys. Rev. Lett. **93**, 183201 (2004); C. A. Stan *et al.*, Phys. Rev. Lett. **93**, 143001 (2004).

[14] S. Kotochigova, P. S. Julienne, and E. Tiesinga, Phys. Rev. A **68**, 022501 (2003).

[15] V. A. Yurovsky *et al.*, Phys. Rev. A **62**, 043605 (2000).

[16] T. Mukaiyama *et al.*, Phys. Rev. Lett. **92**, 180402 (2004).

[17] B. Damski *et al.*, Phys. Rev. Lett. **90**, 110401 (2003).

[18] T. Bergeman *et al.*, Eur. Phys. J. D **31**, 179 (2004).

[19] W. C. Stwalley, Eur. Phys. J. D **31**, 221 (2004).

[20] S. Kotochigova, E. Tiesinga, and P. S. Julienne, Eur. Phys. J. D **31**, 189 (2004).

[21] G. Igel-Mann *et al.*, J. Chem. Phys. **84**, 5007 (1986); S. Kotochigova (private communication).

[22] H. R. Thorsheim, J. Weiner, and P. S. Julienne, Phys. Rev. Lett. **58**, 2420 (1987); F. Masnou-Seeuws and P. Pillet, Adv. At. Mol. Opt. Phys. **47**, 53 (2001).

[23] D. E. Cooper, C. M. Klimcak, and J. E. Wessel, Phys. Rev. Lett. **46**, 324 (1981).

[24] C. E. Fellows *et al.*, J. Mol. Spectrosc. **197**, 19 (1999).

[25] A. J. Kerman *et al.*, Phys. Rev. Lett. **92**, 033004 (2004).

[26] W. Ketterle *et al.*, Phys. Rev. Lett. **70**, 2253 (1993).

[27] M. H. Anderson *et al.*, Phys. Rev. A **50**, R3597 (1994).

[28] Th. Weber, E. Riedle, and H. J. Neusser, J. Opt. Soc. Am. B **7**, 1875 (1990).

[29] G. He *et al.*, J. Opt. Soc. Am. B **7**, 1960 (1990).

[30] R. Sussman, R. Neuhauser, and H. J. Neusser, J. Chem. Phys. **100**, 4784 (1994).

[31] The UPM production rate is calculated assuming 8% ionization efficiency. This value was derived by comparing the signal from the ionization of $a(v = 37)$ molecules with the predicted rate of $a(v = 37)$ production [25]. The inferred efficiency is consistent with claims of other groups operating under similar conditions; see, e.g., C. Drag *et al.*, IEEE J. Quantum Electron. **36**, 1378 (2000).

[32] H. Lefebvre-Brion and R. W. Field, *The Spectra and Dynamics of Diatomic Molecules* (Elsevier, San Diego, 2004).

[33] T. Takekoshi, J. R. Yeh, and R. J. Knize, Opt. Commun. **114**, 421 (1995).

[34] T. Takekoshi and R. J. Knize, Opt. Lett. **21**, 77 (1996).

[35] A. Mosk *et al.*, Appl. Phys. B **B73**, 791 (2001).

[36] T. Takekoshi, B. M. Patterson, and R. J. Knize, Phys. Rev. Lett. **81**, 5105 (1998).

[37] B. Friedrich and D. Herschbach, Phys. Rev. Lett. **74**, 4623 (1995); P. Braun and A. Petelin, Sov. Phys. JETP **39**, 775 (1974).